

SMALL-SCALE STRUCTURE IN THE GALACTIC ISM: IMPLICATIONS FOR GALAXY CLUSTER STUDIES

JOEL N. BREGMAN¹, MEGAN C. NOVICKI², JESSICA E. KRICK¹, AND JOHN S. ARABADJIS³
Draft version February 25, 2009

ABSTRACT

Observations of extragalactic objects need to be corrected for Galactic absorption and this is often accomplished by using the measured 21 cm HI column. However, within the beam of the radio telescope there are variations in the HI column that can have important effects in interpreting absorption line studies and X-ray spectra at the softest energies. We examine the HI and DIRBE/IRAS data for lines of sight out of the Galaxy, which show evidence for HI variations in of up to a factor of three in 1° fields. Column density enhancements would preferentially absorb soft X-rays in spatially extended objects and we find evidence for this effect in the *ROSAT PSPC* observations of two bright clusters of galaxies, Abell 119 and Abell 2142.

For clusters of galaxies, the failure to include column density fluctuations will lead to systematically incorrect fits to the X-ray data in the sense that there will appear to be a very soft X-ray excess. This may be one cause of the soft X-ray excess in clusters, since the magnitude of the effect is comparable to the observed values.

Subject headings: ISM: structure – X-rays: galaxies: clusters: ISM

1. INTRODUCTION

In the course of analyzing X-ray observations of extragalactic objects, corrections are applied for the effects of Galactic absorption. The amount of Galactic absorption can be fit directly from the observations for adequately strong sources with a known underlying spectrum, and this value can be compared to the amount of HI measured from 21 cm line emission. The similarity or difference between these two measures of the absorption column can be used for a variety of purposes, such as to examine whether there is excess absorption within a cluster of galaxies (White et al. 1991; Arabadjis & Bregman 2000) or whether absorption by molecular material is commonplace within the Galaxy (Arabadjis & Bregman 1999a). In other cases, one can fix the X-ray absorption column at the 21 cm HI value and examine whether there is an additional emission component in a system, such as the very soft X-ray excess (the EUVE excess) that has been claimed to exist in clusters of galaxies (e.g., Lieu, Bonamente & Mittaz (1999); but see Bowyer, Berghöfer & Korpela (1999) and Arabadjis & Bregman (1999b)).

In these studies, one usually ignores the small-scale structure of the neutral Galactic ISM, assuming that the mean 21 cm column density within a radio telescope beam is uniform across the face of the beam, which is typically 30' for the single-dish radio telescopes that most of the HI values are based upon. Naturally, there is structure to the total neutral column within the radio telescope beam and this has the potential of influencing the analysis of extragalactic X-ray emission as well as absorption studies in the optical and ultraviolet region. Here we examine the magnitude of the variation of the small-scale structure in the neutral Galactic layer and we discuss the implications for the analysis of data. First, we present an idealized model

to illustrate the magnitude of the effect (§2), and then we present the HI and X-ray observations that show the magnitude of the variation in the absorption column (§3, 4). Among other effects, we show that by ignoring such structure in the ISM, absorption corrected X-ray spectra of clusters will systematically show an apparent excess soft emission component, of the sort that is seen in some EUVE observations of galaxy clusters (§5).

2. AN EXAMPLE OF THE IMPORTANCE OF SMALL-SCALE STRUCTURE

The importance of small-scale structure on absorption corrections can be illustrated by adopting simple models for the fluctuations in N_H that are sensible and are consistent with the observations discussed below. In one model, we assume that the column density distribution $f(N)$ has a minimum level, N_{low} , a maximum level, N_{high} , and behaves as a power-law between these levels so that

$$\begin{aligned} f(N) &= N^{-m} & \text{for } N_{low} \leq N \leq N_{high} \\ f(N) &= 0 & \text{for } N < N_{low}, N_{high} < N \end{aligned} \quad (1)$$

The mean column density is the 21 cm HI column, which is

$$\begin{aligned} N_{avg} = N_{21cm} &= \frac{\int_{N_{low}}^{N_{high}} f N dN}{\int_{N_{low}}^{N_{high}} f dN} \\ &= \frac{m-1}{m-2} \left(\frac{N_{low}^{-(m-2)} - N_{high}^{-(m-2)}}{N_{low}^{-(m-1)} - N_{high}^{-(m-1)}} \right), \end{aligned} \quad (2)$$

and in the case of $N_{high} = \infty$, we have the simple form $N_{21cm} = \frac{m-1}{m-2} N_{low}$. For individual lines of sight out of the Galaxy, one is more likely to measure a column that is typically closer to the median column density rather than the

¹ University of Michigan, Department of Astronomy, 833 Dennison Building, Ann Arbor, MI 48109

² Institute for Astronomy, University of Hawaii, 2680 Woodlawn Drive, Honolulu, HI 96822

³ Massachusetts Institute of Technology, Center for Space Research, 70 Vassar Street, Room 37-501, Cambridge, MA 02139

average column density N_{avg} . The median column density, or the column density most often be sampled, is

$$N_{median} = 2^{1/(m-1)} (N_{low}^{-(m-1)} + N_{high}^{-(m-1)})^{-1/(m-1)} \quad (3)$$

and in the limit of $N_{high} = \infty$, $N_{median} = 2^{1/(m-1)} N_{low}$. Then, the ratio of the median to the mean is, in the limit of $N_{high} = \infty$,

$$N_{median}/N_{21cm} = \frac{(m-2) 2^{1/(m-1)}}{m-1}. \quad (4)$$

If the distribution function were infinitely sharply peaked, $N_{median} = N_{21cm}$, but if the distribution has some significant width, these two quantities can be measurably different. For example, with a value of $m = 3.5$, consistent with the data of Wakker, Oosterloo & Putman (2002), $N_{median}/N_{21cm} = 0.792$, or about a 20% difference between the median and the mean. This implies that individual lines of sight out of the Galaxy will generally return a value for the column that is about 20% lower than the column induced from the 21 cm measurements. As an example of the importance of this in an astrophysical setting, this phenomenon will affect the interpretation of absorption line measurements (single lines of sight) when they are compared to the amount of 21 cm emission (as was first pointed out to us by Wakker). In a comparison of a Ly α absorption line to a 21 cm emission line measurement, one would find the systematic effect that the absorption column was less than the emission column. In the determination of metallicities that compare metal absorption lines to 21 cm emission, one would determine a lower than true metallicity more often than a higher metallicity.

These small scale variations in the HI column will affect the absorption of light in the X-ray waveband in significant ways, especially at high optical depths. The transmitted fraction of light at some energy is given by

$$Tr(E) = I_o(E) \frac{\int e^{-\sigma(E)N(x,y)} dx dy}{\int dx dy} \quad (5)$$

At low optical depth ($\tau(x, y, E) = \sigma(E)N(x, y) \ll 1$, where $\sigma(E)$ is the energy dependent cross section), this just reduces to $Tr(E) = I_o(E)(1 - \sigma(E)N_{avg})$, so it is appropriate to use $N_{avg} = N_{21cm}$, as is usually done. However, if there are variations in $N(x, y)$ when $\tau > 1$, the effective X-ray absorption column changes with energy, with the deviation from N_{21cm} becoming greater toward lower energies, which is the direction of increasing optical depth. This can be illustrated in Figure 1, where we show the transmitted fractions as a function of energy for the case where $N_{avg} = N_{21cm} = 2 \times 10^{20} \text{ cm}^{-2}$, and where the variation occurs from $N_{low} = 0.82 N_{avg}$ to $N_{high} = 1.31 N_{avg}$, with $m = 3.5$. At high optical depths, the transmission is underestimated when using N_{21cm} . The reason is due to the non-linearity in the behavior of the transmission with column, so that the fluctuations toward low density (lower optical depth) permit far more photons to flow through than an equivalent high density fluctuation removes. This leads to a residual flux when fitting a model with constant N_{21cm} to the data, and this positive residual is a systematic effect that is prominent in a moderately narrow energy range where $4 \gtrsim \tau \gtrsim 1$. The absolute value of the residual is small at low energies because the optical depth through the Galaxy is large, while the residual

vanishes at larger energies because the optical depth becomes low enough that using a constant N_{21cm} is a good approximation. This effect can be rather important in the discussion of the reality of the soft excess X-ray emission, as we discuss below. However, first it is important to understand the magnitude of the fluctuations in N so that the importance of the effects can be assessed.

3. THE MAGNITUDE OF SMALL-SCALE STRUCTURE IN THE ISM FROM 21 CM STUDIES

Most extragalactic objects that have been studied lie at Galactic latitudes $b > 20^\circ$, or lines of sight that are out of the plane of the Milky Way. For such lines of sight, there are few studies of the small-scale structure in the total HI column, and almost no information on the structure of H₂. The type of information needed is the distribution function of column densities within the larger beam of single-dish surveys (i.e., a histogram of N_{HI}). In principle, this can be obtained with synthesis arrays, but such instruments normally resolve away the larger scale structure, showing only small-scale variations. However, synthesis array observations, used in conjunction with single-dish observations (the zero spacing data) can recover all the emission and show the true distribution of N_{HI} . Unfortunately, few such observations have been made out of the plane, although there are many such observations in the plane, which show a rich amount of structure. Out of the plane, two published observations are by Wakker, Oosterloo & Putman (2002), which is toward a high velocity cloud (WW 187) in the direction of NGC 3783, $l = 287^\circ$, $b = 23^\circ$, and by Joncas, Boulanger & Dewdney (1992), which is toward a filament of far infrared cirrus emission at $l = 141^\circ$ $b = 30^\circ$. Although these may not be typical regions, we examine them since they provide a starting point for understanding small-scale structure; we will be obtaining 21 cm data toward more typical sight lines in the near future.

The observation by Joncas, Boulanger & Dewdney (1992) is toward a gas and dust complex in Ursa Major that has conspicuous IR-cirrus emission and is also known to have some molecular gas. However, the mean HI column in this direction is $3.4 \times 10^{20} \text{ cm}^{-2}$, which is fairly typical for sight lines at this Galactic latitude. The observation was made with the Synthesis Radio Telescope of Dominion Radio Astrophysical Observatory, including zero spacing data and complementary observations in the continuum; the resulting resolution was $1'$ and the field of view was 2.6° . Since the sensitivity is dropping toward the edges, and the absolute calibration suffers, we have chosen to look at the variations in the central 1° region, smoothed to $2.3'$ and formed a histogram of the column densities (Figure 2). There is a fairly sharp cutoff in $N(\text{HI})$ for values below $1.7 \times 10^{20} \text{ cm}^{-2}$, but there is a distribution that extends to $5.9 \times 10^{20} \text{ cm}^{-2}$, a range of almost a factor of four (0.54 in the log).

The observation by Wakker is of a HVC projected upon a background AGN (NGC 3783) in the Southern Hemisphere, for the purpose of understanding the optical and ultraviolet absorption line results toward NGC 3783. The synthesis observations were made with the Australia Telescope Compact Array, supplemented with data from the Parkes Multibeam survey, so that HI structures were not

resolved out of the image. The map that they produced was not of all of the Galactic HI in that region, but only the HI in the velocity range surrounding cloud, or 190-280 km s⁻¹. Although it would be better to have the entire Galactic column, such a map was not produced, so we have analyzed the existing map, which should give us some insight into HI variations. We have used a square box 1° on a side located in the central region in order to determine the column density histogram (Figure 3), which shows that there is a sharp drop in the column below 0.65×10^{20} cm⁻². The HI distribution is moderately flat to 1.2×10^{20} cm⁻², declining toward higher values (16×10^{20} cm⁻² in a way that may be described as a broken power-law of slopes -3 to -4 (or with an exponential model). A detailed analysis of this distribution is given in Wakker, Oosterloo & Putman (2002).

Although there are few HI maps such as the above, the entire sky has been mapped in the far infrared with DIRBE and IRAS data by Schlegel, Finkbeiner & Davis (1998). These authors have produced maps of $E(B-V)$, which are, on average, proportional to the HI column density, and with 2.67' resolution. We sampled five randomly chosen 1° square regions located at $l, b = -141.3^\circ, 37.3^\circ; 14.0^\circ, 74.8^\circ; 112.8^\circ, 47.7^\circ; -44.3^\circ, 45.4^\circ; \text{ and } 52.4^\circ, 55.9^\circ$, and analyzed the column density distribution, using the relationship of $N(HI) = 8.18 \times 10^{21} E(B-V) + 2.54 \times 10^{19}$ cm⁻², which was determined by us using other lines of sight out of the Galaxy. It is evident that the full range is at least 100% relative to the minimum value (Figure 4). However, we can better characterize the range by using the quartile points, referenced to the median column density, which in percentage, is $100(N(75\%) - N(25\%))/N_{median}$, where $N(75\%)$ and $N(25\%)$ are the columns at the 75% and 25% quartile locations. Using this measure, we find that for these selected regions, the range is fairly narrow, 14.6-19.2% with an average value of 16.5%.

Unfortunately, it is nearly impossible to determine whether the degree of fluctuations seen in the HI is the same as in the IRAS-DIRBE data at a resolution of 1'. The HI data from Wakker show a greater degree of HI fluctuations than does the IRAS-DIRBE data, but this may be because the HI map does not include HI at all velocities. In the region studied by Joncas, the HI and IRAS-DIRBE variations are similar in magnitude, but this region was chosen because of the prominent IRAS structure in the field, which guarantees substantial variation. One might expect the IRAS-DIRBE variations to be smaller than the HI variations just because the "beam" of the IRAS-DIRBE data is an order of magnitude larger than the HI radio synthesis beam of about 1' (so small scale variations are washed out). This is an issue where more data would be extremely valuable.

There is additional evidence for small-scale structure in the interstellar medium, such as from the studies that are based upon optical and ultraviolet absorption measurements. The studies of NaI absorption systems toward globular cluster stars show that there are variations in the equivalent width by a factor of a few on scales of 1-4' (Langer, Prosser & Sneden 1990) as well as on scales of $\sim 10''$ (Andrews, Meyer & Lauroesch 2001). Absorption line studies toward binary stars show that there is significant structure in the ISM on a scale of 0.1'' (Laroesch,

Meyer, and Blades 1999). In addition, HI absorption studies of the 21 cm line show that 10-15% of cold HI occurs on scales below 0.1''. Frail et al. (1994) study the changes in 21 cm absorption toward pulsars with known velocities, detecting changes in the absorption line over a timescale of a few years, which corresponds to a change of 10-100 mas. On comparable angular scales, Faison et al. (1998) used VLBI studies toward radio AGNs and find variations in the HI optical depth as large as a factor of two. Unfortunately, neither the optical absorption lines (NaI, KI) or the 21 cm absorption line is a true linear indicator of the gas column because the optical metal lines can be sensitive to changes in the ionization state while the 21 cm optical depth is inversely proportional to the temperature. Nevertheless, these studies are consistent with the presence of structure in the interstellar column on relatively small scales.

4. SMALL-SCALE VARIATION FROM X-RAY OBSERVATIONS

The absorption of soft X-rays depends upon the column of intervening gas as well as the energy of the observation, since the approximate relationship for the optical depth is $\tau \propto NE^{-3}$, where N is the column of X-ray absorbing gas (usually expressed as an equivalent HI column) and E is the energy of the photons. For a column density of $N = 2 \times 10^{20}$ cm⁻², $\tau = 1$ at 0.24 keV, while for a column of 4×10^{20} cm⁻², $\tau = 1$ occurs at 0.32 keV, so if there are significant fluctuations in the X-ray absorption column, we should see a "drop-out" of the soft emission (the ratio of soft to hard emission decreases). At these column densities, the absorption of X-rays is due primarily to HeI, with HI being the second most important absorber. Other components of the ISM are less important as absorbers (warm ionized gas or hot X-ray emitting gas), so the X-ray column is a fairly good measure of the neutral column.

This effect is, in principle, possible to detect against a relatively smooth extended extragalactic X-ray emitting object such as a cluster of galaxies. In practice, it is possible to search for this effect only in clusters of high surface brightness and for the correct range of Galactic column density, at least when using ROSAT data. The ROSAT PSPC data has rather limited energy resolution so that the data can only be separated into a two or three independent spectral regions. One of these divisions is due to the presence of carbon in the optical path, which leads to a sharp absorption edge at 0.284 keV that becomes progressively less important at higher energies. Operationally, this leads to a local minimum in the detection efficiency near 0.5 keV, so we have divided the PSPC data into two bands, 0.2-0.5 keV and 0.5-2.0 keV (PI channels 20-51 and 52-201). Snowden et al. (1994) have developed procedures to extract diffuse emission in various energy bands, corrected for point sources, instrumental background, and local background sources (solar scattered X-rays, etc.). Here we use those procedures to form the ratio of band R2+R3 (the 0.2-0.5 keV band) to R4+R5+R6+R7 (0.5-2.0 keV).

In order to detect variations in the ratio of these two bands, there must be sufficient photons in the soft band for statistical reasons and that implies a mean Galactic absorption column of less than about 6×10^{20} cm⁻² (otherwise there are no soft photons) but the absorption in the

soft band should be significant ($\tau = 1$) so that modest variations in τ lead to detectable variations in the X-ray ratio. For example, if the mean Galactic column is $3 \times 10^{20} \text{ cm}^{-2}$ and there is a region where the column rises to $4 \times 10^{20} \text{ cm}^{-2}$, our hardness ratio will decrease by 30% while if there is a region where the column rises to $5 \times 10^{20} \text{ cm}^{-2}$, the hardness ratio will drop to half its original value. From the above discussion, variations of this sort are not likely, although the probabilities of finding such variations can depend strongly on region. For the HI data of Joncas, Boulanger & Dewdney (1992) and Wakker, Oosterloo & Putman (2002) about 20% of the data are above the mean by 4/3 and 10% of the data are above the mean by a factor of 5/3 or greater. However, if one uses the variations in the DIRBE/IRAS data for these two regions and the five other regions (above), typically only 1% of the area has an intensity value that is above the mean by 4/3 or greater. Since the variation in the DIRBE/IRAS data is less than that in the HI for the region observed by Wakker, Oosterloo & Putman (2002), this latter value of 1% may be an underestimate. This suggests that finding significant variation in our hardness ratio is likely if there are several hundred independent positions.

We analyzed five clusters as given in Table 1, all of which are bright nearby systems that are fairly symmetrical in their inner $6'$. The X-ray temperatures and the bolometric luminosities are taken from Wu, Xue & Fang (1999), for $H_0 = 75 \text{ km s}^{-1} \text{ Mpc}^{-1}$, and the HI columns are those given by Dickey & Lockman (1990).

[EDITOR: INSERT TABLE 1 HERE.]

Because galaxy clusters have radial temperature gradients, which would lead to radial softness variation, we examined softness variations azimuthally, either in circular annuli, or in the case of clusters with elliptical isophotes, in elliptical annuli. We avoided the central region and used four annular regions with radii (or semi-major axis) of $1'-2'$ (annulus 1), $2'-3'$ (annulus 2), $3'-4.25'$ (annulus 3) and $4.25'-5.5'$ (annulus 4). We also examined larger annuli, but the surface brightness was generally too low to be of use. In addition, each annular region was divided into 24 regions of 15° each, with region 1 being from position angle 0° to 15° , with the position angle increasing east from north as is the usual convention. This leads to 96 independent positions per cluster.

The signature that we are looking for in the X-ray emission is a local hardening of the emission due to the soft photons being absorbed by an excess in the Galactic HI. This will lead to a decrease in the hardness ratio with the change due to decrease in the number of soft photons rather than an increase in the number of hard photons. We discuss each of the systems in turn.

Abell 119: The hardness ratio is shown as a function of annular ring and region (position angle) in Figure 5. There are three positions for which the hardness ratio is more than 3σ from the mean of the sample (annulus 1, region 2; annulus 2, region 19; annulus 3, region 8). In each case, the deviation is in the sense that the region is harder than the mean and it is the soft band that has decreased relative to its neighbors rather than an increase in the hard band. These are precisely the expectations for regions with excesses in their Galactic HI columns. Also, the next four deviant points in the sample (about 2.5σ ;

regions 6, 11, and 22 in annulus 3 and region 4 in annulus 4) are also harder than the average and due to a decrease in the number of soft photons.

Abell 209: There is one region that deviates by more than 3σ and is in annulus 1 at region 10, but this is due to a positive deviation in the hard flux rather than a decrease in the soft flux, so this does not meet our criteria.

Abell 2142: In this system, we used elliptical isophotes with an eccentricity of 0.82 and an orientation of the major axis of -58° . There is a strong point source that could not be removed and it affects the first three regions in annuli 2, 3, and 4 (at PA $0-45^\circ$), so they were removed from the analysis. The photon statistics were good for this long observation, so the annuli were divided into 30 regions, each 12° wide. There are two regions with deviations more than 3σ (annulus 2, region 26; annulus 3, region 8), both regions being harder than the average and the hardness is due to the lack of soft photons rather than an excess of hard photons (Figure 6).

For the remaining two systems, AWM4 and Abell 3376, there was no evidence of deviations in the hardness ratio beyond 3σ , although the numbers of photons were less than the other clusters, so the statistical significance is poorer.

To summarize, there were about 600 locations in which we could have seen fluctuations in the hardness ratio, although about half those were of lower statistical quality than the others. Six locations deviated from the mean hardness ratio in their annuli by more than 3σ , all toward the region of fewer soft photons. About one such deviation is expected from statistical fluctuations, so this represents an excess. Five of these six regions were harder because of a paucity of soft photons, as would be expected if there were a positive excess in the Galactic neutral hydrogen column. We cannot rule out that these statistically meaningful fluctuations in the hardness ratio is intrinsic to the cluster. To determine whether the fluctuations are due to variations in the Galactic gas will require an accurate HI map in this region. In addition, we will be able to more accurately define the hardness variations with future X-ray observations, especially with XMM-Newton.

Although point sources are largely removed in the data processing, we comment on the effect by point sources that are unresolved and therefore would not be removed. In the ROSAT band, the typical point source is of comparable hardness to the thermal Bremsstrahlung X-ray emission from a galaxy cluster. Also, the surface brightness of a galaxy cluster is much greater than that of the unresolved X-ray background sources. Taken together, we expect that unresolved point sources will not influence our analysis.

5. APPLICATIONS

The fluctuations in the foreground absorption column can have a number of effects, each of which should be modeled. These fluctuations can lead to variable absorption and reddening, which will affect the properties of an HR diagram of a star cluster. Another example occurs in absorption line studies (as discussed above), since the mean neutral gas column inferred from 21 cm emission studies is likely to be higher than the median line of sight, which is more relevant for individual lines of sight. A third example, which we explore in more detail, is the modeling

of galaxy clusters, since this will be a systematic effect. This systematic effect either leads one to obtain an X-ray absorption column lower than the mean column (which would help explain the results of Arabadjis & Bregman (1999b), or alternatively, it will lead to a flux residual that might be attributed to a new "soft" component of the X-ray emission.

The presence of a new soft X-ray component was first presented by Lieu et al. (1996) from data obtained with the EUVE satellite, combined with ROSAT X-ray data. The instrument used by the EUVE for this detection was the DS telescope (Boyer & Malina 1991), which is sensitive to photons up to about 0.19 keV, which is the soft X-ray region. Soft X-rays can be absorbed by Galactic gas, and for a moderately low column density of $2 \times 10^{20} \text{ cm}^{-2}$, the optical depth to continuous absorption is unity at 0.24 keV and $\tau = 3$ at 0.16 keV, so the X-rays that are detected in the EUVE band lie in the heavily absorbed region of the X-ray spectrum. Lieu et al. (1996) took the X-ray spectrum of some bright galaxy clusters and fit an absorption spectrum with a single column density and then compared the flux in the EUVE band to the measured value. They found that the EUVE emission was brighter than anticipated, leading them to conclude that there was a very soft X-ray excess in the emission that needed to be explained.

The validity of this emission has been questioned from two other works on the subject. Arabadjis & Bregman (2000) pointed out that the same soft excess should be visible in the ROSAT PSPC as well, and possibly easier to detect. The effective areas of the PSPC and the EUVE DS telescope are shown in Figure 7, which includes not only the raw collecting area of both instruments, but the effective collecting area due to absorption by Galactic gas with a column density of $2 \times 10^{20} \text{ cm}^{-2}$, which is fairly typical of the sight lines involved. One finds that the effective EUVE bandpass is 0.144-0.186 keV (FWHM), which can be a great aid because although the PSPC has more effective collecting area in this energy range, its energy resolution is significantly poorer than the EUVE bandpass of 0.04 keV. In this EUVE bandpass, the optical depth is about 3, so if the Galactic column has been overestimated slightly, it makes a large difference in the predicted flux. Galactic columns out of the plane, such as these, are difficult to determine accurately, and Arabadjis & Bregman (1999b) showed that in nearly all cases, the soft X-ray excess would vanish if one adopted a column that was less than 3σ from the published values. The only exception was the Coma cluster, for which the Galactic column is particularly small. For low HI columns, the corrections to the 21 cm observations are the greatest, so it is possible that the HI column is particularly low and that there is no soft X-ray excess.

The validity of the soft X-ray excess was also questioned by Bowyer, Berghöfer & Korpela (1999), who showed that certain data processing issues could complicate the ability to analyze the data. In particular, they showed that flat-fielding was a key issue, so they constructed flat fields from many long observations, and when this was applied, soft excesses vanished in Abell 2199 and Abell 1795, two clusters that Lieu, Bonamente & Mittaz (1999) claimed to have excesses. However, they find that the Coma cluster still has an excess in its soft X-ray emission, the same re-

sult as Arabadjis & Bregman (1999b), working from the ROSAT data.

Here we show that even if one has measured the mean Galactic 21 cm column correctly, fluctuations in that HI column lead to a soft X-ray excess. As an example, when we use the model described in §2, the residual flux has a peak at about 0.19 keV and a substantial amount of flux falls in the EUVE band (Figure 8). In the EUVE band, the fractional excess is claimed to be about 20-50% above the expected values, and that is approximately the amount that we predict from our model of column density fluctuations (Figure 9).

Ideally, one should use the detailed column density map associated with the particular clusters in question, but 21 cm data of this sort does not exist. Consequently, we cannot demonstrate that this effect is responsible for the extraction of a soft X-ray excess; we merely suggest it as a possibility.

6. DISCUSSION AND FINAL COMMENTS

We have shown the potential implications of variations in the Galactic absorption column in trying to interpret a variety of observations. The greatest shortcoming in determining the true importance of this effect is the lack of accurate data on the HI variations on the sky at small angular scale. Such observations need a combination of synthesis array observations in combination with single dish data in order to include the "zero spacing" data. Aside from the two observations discussed above, data of this kind have been largely confined to the Galactic plane, where the Dominion Radio Astronomy Observatory has undertaken a survey from $74^\circ < l < 147^\circ$, but in the narrow latitude band $-3.5^\circ < b < 5.5^\circ$. This is far from the region where most of the galaxy clusters lie, typically $20^\circ < |b|$.

Another issue that needs to be examined is the degree to which the HI fluctuations in these fields follows the DIRBE/IRAS maps of Schlegel, Finkbeiner & Davis (1998). If it could be shown that the HI generally follows the DIRBE/IRAS data to good accuracy, then one could use that data as a proxy for the HI data. Currently, the situation is unclear since in the WW 187 field, there is a poor correlation between the HI column and the DIRBE/IRAS data, while in the IRAS filament mapped by Joncas, the correlation is much better.

There are a variety of effects that will be clarified by future HI observations, so we strongly encourage observers to obtain such data.

We are especially indebted to Bart Wakker and Gilles Joncas for sending us copies of their data for us to analyze. Also, we would like to thank Thomas Berghöfer for his patience in answering our many questions about EUVE data. We would like to thank Jay Lockman, Jimmy Irwin, Renato Dupke, Morton Roberts, and Stu Bowyer for their advice and comments. Partial support for this work has been provided by NASA through LTSA grant NAG5-10765.

REFERENCES

- Arabadjis, J.S. & Bregman, J.N. 1999a, *ApJ*, 510, 806.
 Arabadjis, J.S. & Bregman, J.N. 1999b, *ApJ*, 514, 607.
 Arabadjis, J.S. & Bregman, J.N. 2000, *ApJ*, 536, 144.
 Andrews, S.M., Meyer, D.M. & Lauroesch, J.T. 2001, *ApJ*, 552, L73.
 Bowyer, S., Berghöfer, T.W. & Korpela, E.J. 1999, *ApJ*, 526, 592.
 Bowyer, S., & Malina, R. F. 1991, in *Extreme Ultraviolet Astronomy*,
 ed. R. F. Malina & S. Bowyer (New York: Pergamon), 397.
 Dickey, J. & Lockman, F.J. 1990, *ARAA*, 28, 215.
 Faison, M.D., Goss, W.M., Diamond, P.J. & Taylor, G.B. 1998, *AJ*,
 116, 2916.
 Frail, D.A., Weisberg, J.M., Cordes, J.M. & Mathers, C. 1994, *ApJ*,
 436, 144.
 Joncas, G., Boulanger, F. & Dewdney, P.E. 1992, *ApJ*, 397, 165.
 Langer, G.E., Prosser, C.F. & Sneden, C. 1990, *AJ*, 100, 216.
 Lieu, R., Mittaz, J.P.D., Bowyer, S., Lockman, F.J., Hwang, C-Y. &
 Schmitt, J.H.M.M. 1996, *ApJ*, 458, L5.
 Lieu, R., Bonamente, M. & Mittaz, J.P.D. 1999, *ApJ*, 517, 91.
 Schlegel, D.J., Finkbeiner, D.P. & Davis, M. 1998, *ApJ*, 500, 525.
 Wakker, Bart P., Oosterloo, Tom A., Putman, Mary E. 2002, *AJ*,
 123, 1953.
 White, D.A., Fabian, A.C., Johnstone, R.M., Mushotzky, R.F. &
 Arnaud, K.A. 1991, *MNRAS*, 252, 72.
 Wu, X.-P., Xue, Y.-J. & Fang, L.-Z. 1999, *ApJ*, 524, 22.

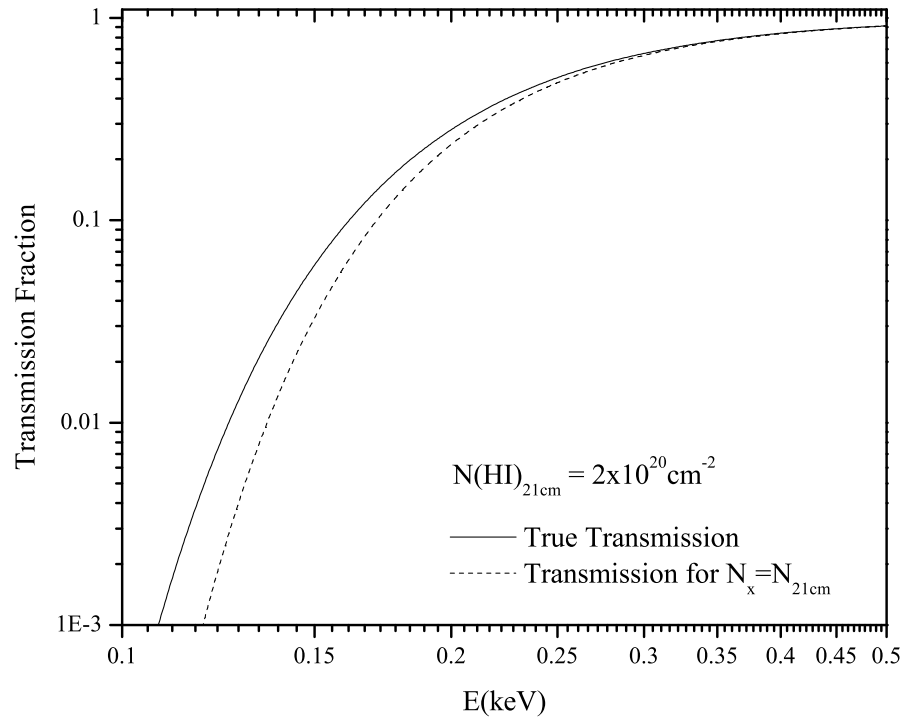


FIG. 1.— The transmission fraction due to neutral atomic gas for a column of $2 \times 10^{20} \text{ cm}^{-2}$ (dashed line) compared to the transmission for gas of the same mean column but with fluctuations as described in the text. The amount of light transmitted through the absorbing medium is less for a uniform absorption column than one that has fluctuations, so the failure to include such fluctuations will lead to a systematic residual at energies where the optical depth exceeds unity.

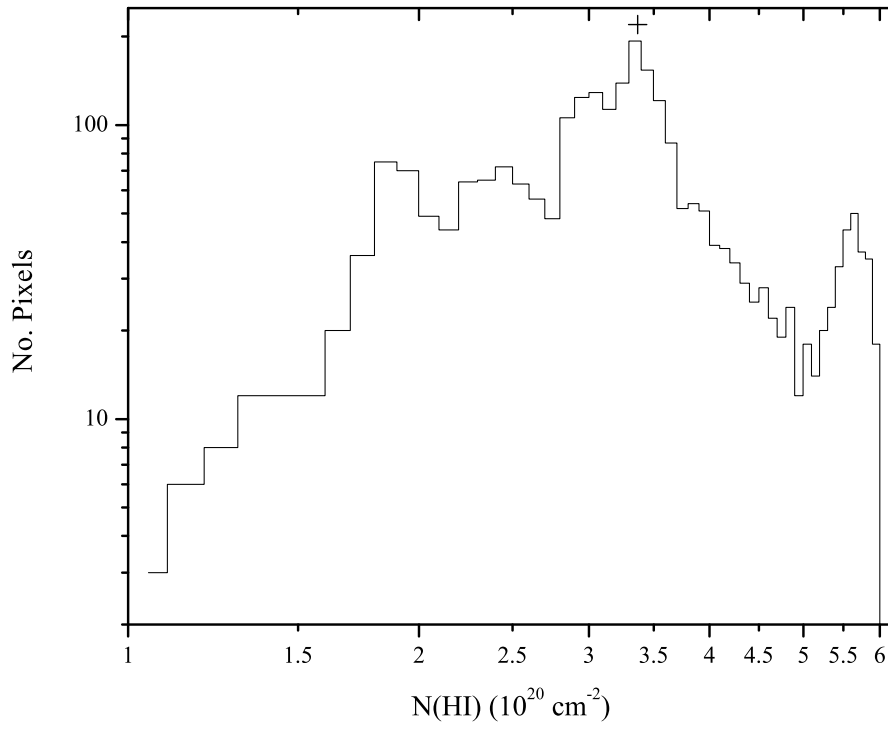


FIG. 2.— Histogram of the HI column density in the central 1° field that was obtained by Joncas et al. (1992). The few very low column density pixels is due to the S/N of the observation (an rms of 5 K). The range in the column density is more than a factor of three in this region, which includes a filament identified in *IRAS* data.

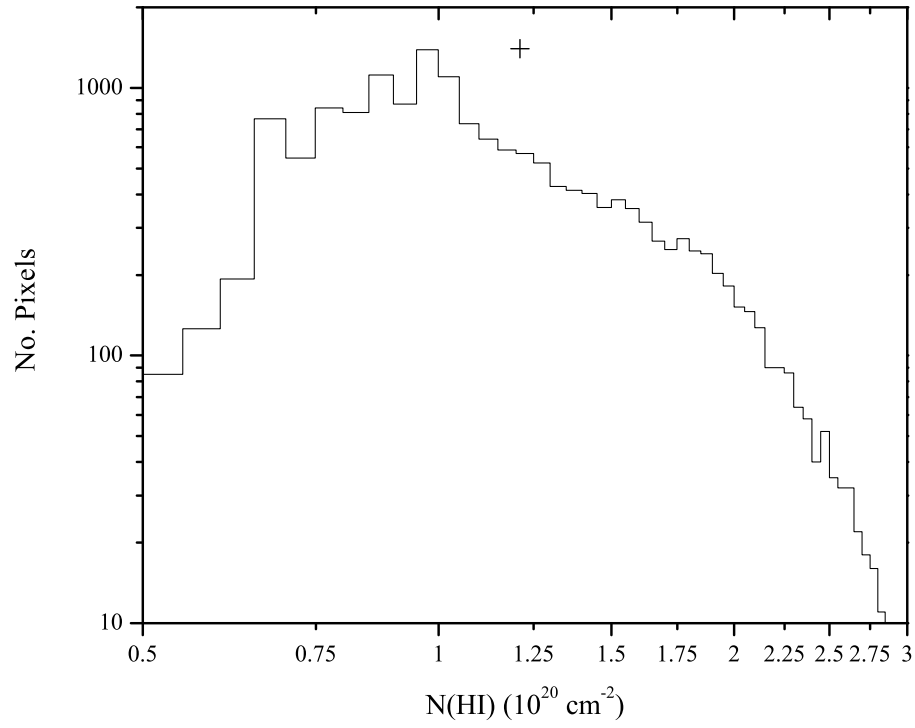


FIG. 3.— Histogram of the HI column density in the field around WW 187 obtained by Wakker, Oosterloo & Putman (2002). A power-law of slope -3.5 would be steeper than the observed distribution for $0.8 \times 10^{20} \text{ cm}^{-2} < N_{21\text{cm}} < 2 \times 10^{20} \text{ cm}^{-2}$, and it would be shallower than the observed distribution at greater columns.

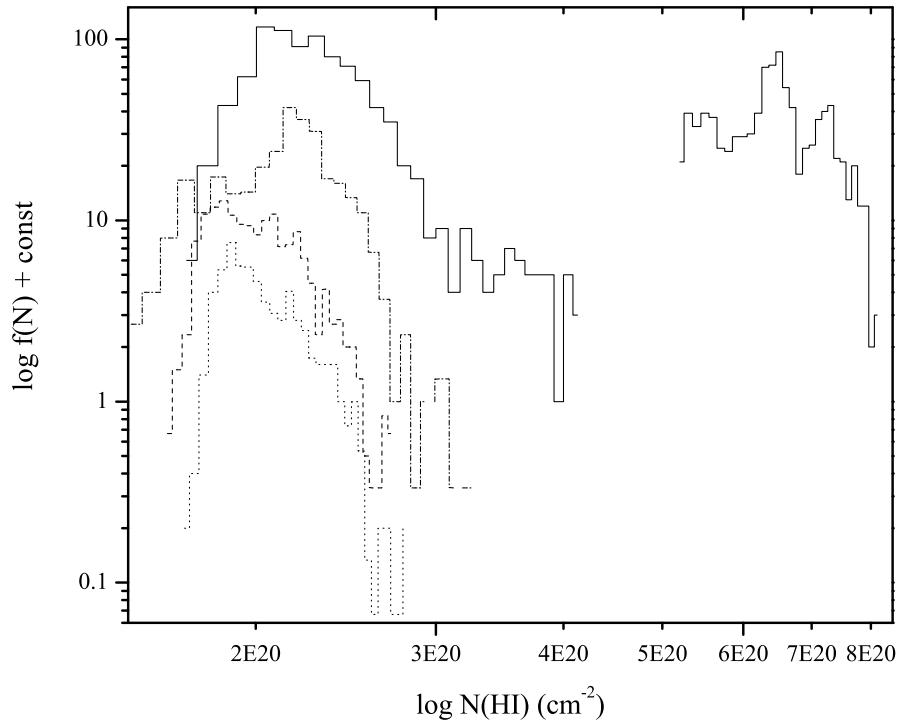


FIG. 4.— The column density distribution within 1° fields inferred from the IRAS-DIRBE data of Schlegel, Finkbeiner & Davis (1998); arbitrary vertical shifts are introduced to separate the histograms. In general, there is a peak in the distribution, with a greater extension to higher column than to lower columns, and in some cases, there is a sharp cutoff at the low column density side.

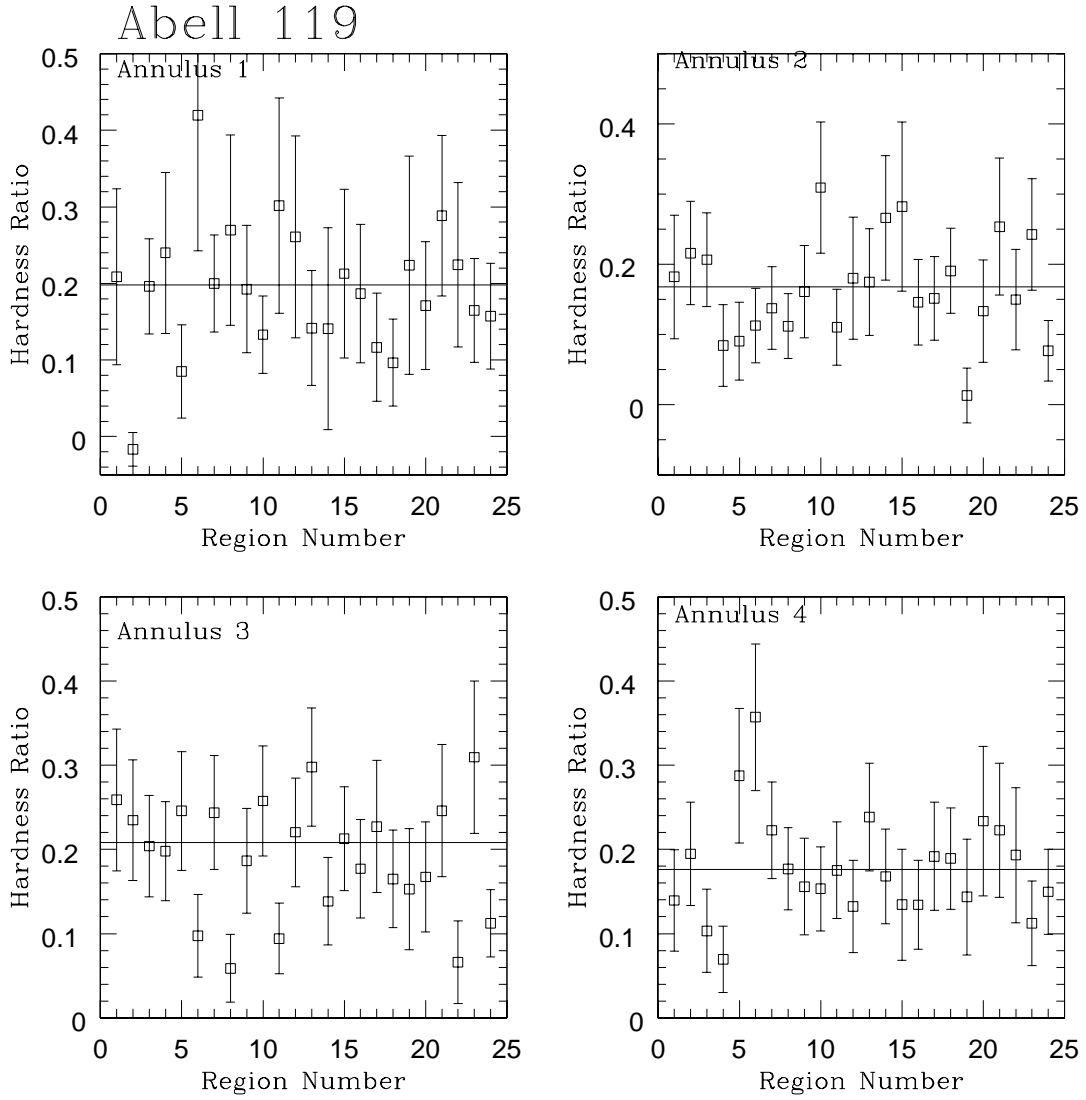


FIG. 5.— The ratio of the fluxes in the 0.2-0.5 keV band to that in the 0.5-2.0 keV band for 15° regions within annuli at $1'-2'$ (annulus 1), $2'-3'$ (annulus 2), $3'-4.25'$ (annulus 3), and $4.25'-5.5'$ (annulus 4), centered on the X-ray center of Abell 119. Several regions have hardness ratios that deviate significantly from the mean, such as at: annulus 1, region 2; annulus 2, region 19; and annulus 3, region 8. Deviations of this nature can be caused by excess gas along the line of sight, which preferentially absorbs the soft X-ray emission.

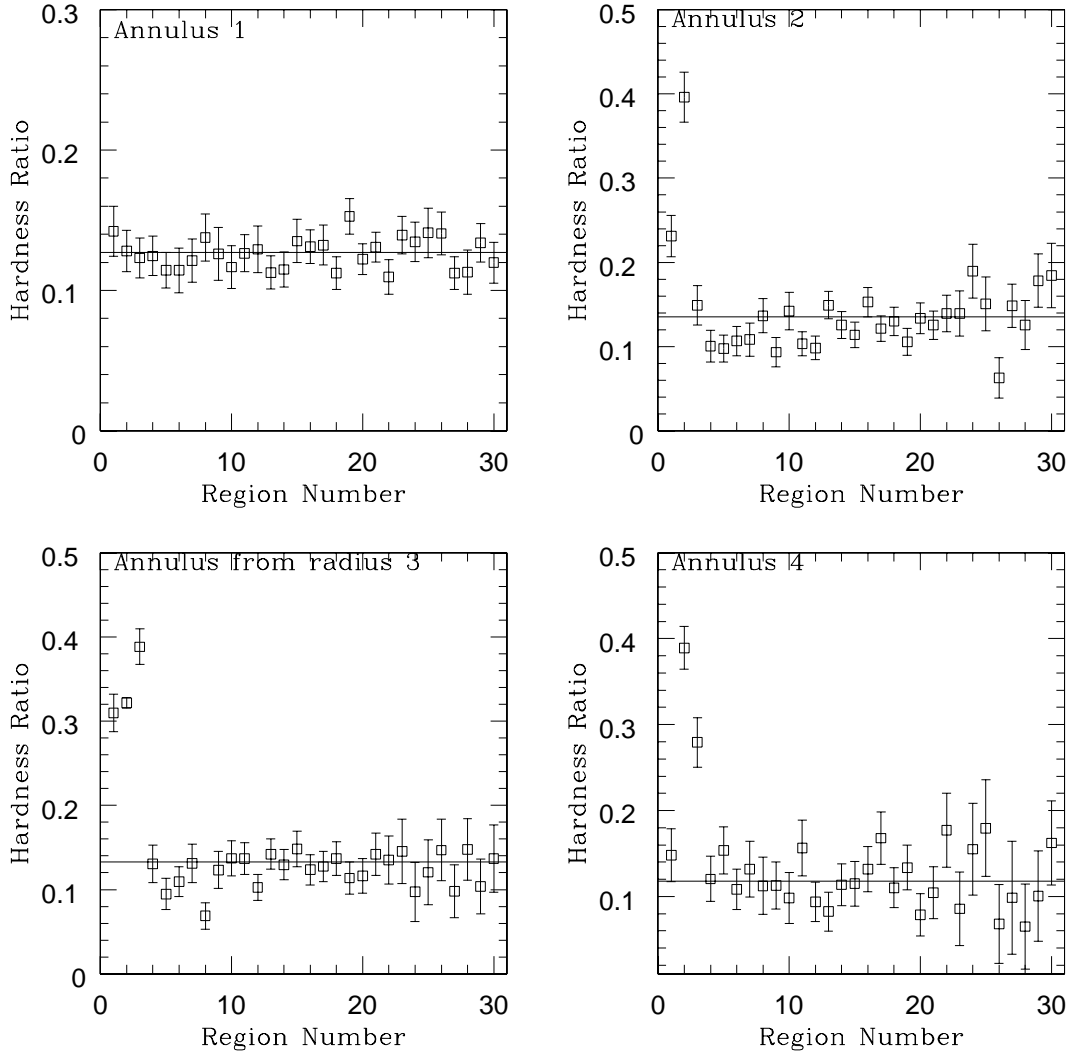


FIG. 6.— The same ratio as in Figure 4, but for elliptical annuli centered on the X-ray center of Abell 2142. There is a strong source of extended emission going from annuli 2-4 in regions 1-3, so these regions were not used in calculating the mean hardness ratio. There are two regions that deviate more than 3σ from the mean (annulus 2, region 26; annulus 3, region 8) and they are harder, consistent with excess absorption by foreground gas.

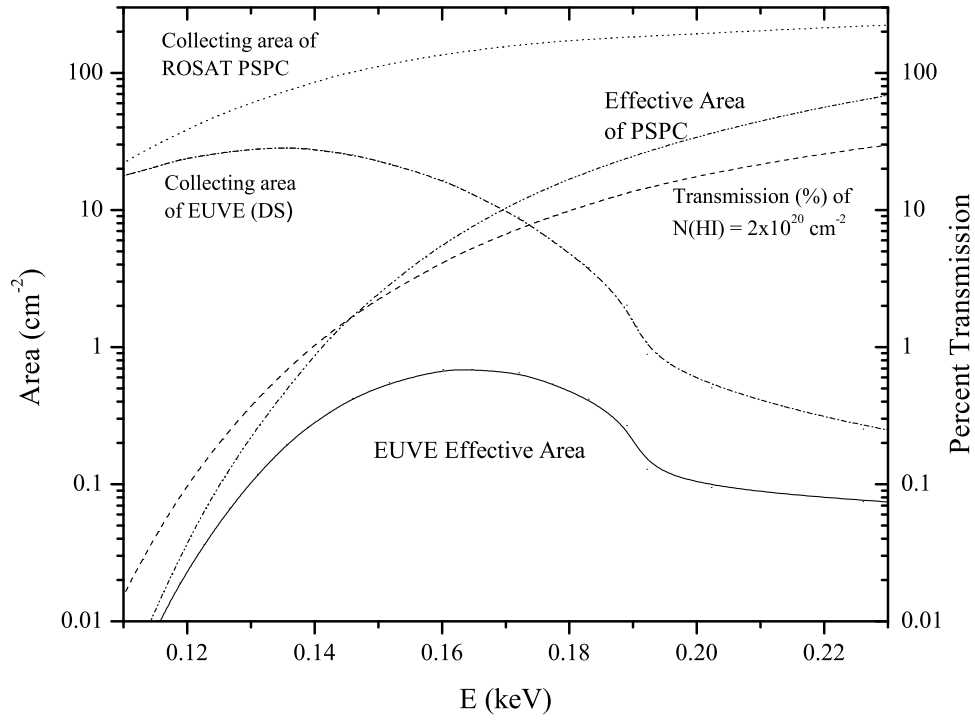


FIG. 7.— The raw and effective collecting areas for the EUVE DS telescope and the ROSAT PSPC in the energy range 0.11 - 0.23 keV. The effective area is the product of the raw collecting area and the fractional transmission through a Galactic gas column of $2 \times 10^{20} \text{ cm}^{-2}$. The EUVE effective area has a bandwidth of about 0.14-0.19 keV (FWHM), so it samples a well-defined waveband, but it has an order of magnitude less effective collecting area than the ROSAT PSPC.

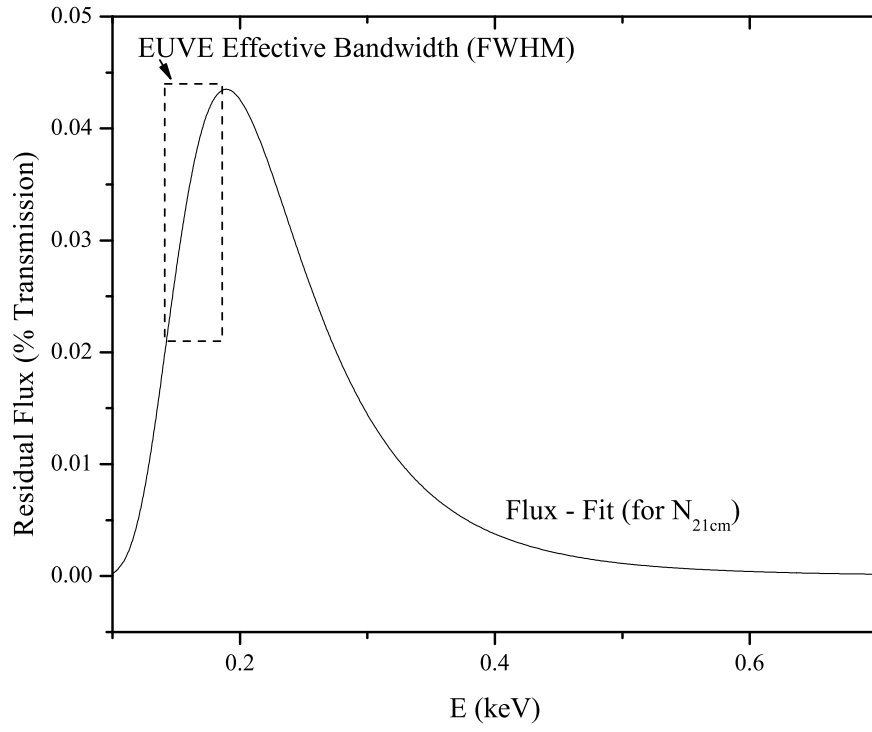


FIG. 8.— The residual between the incident flux and the model for the flux when using the mean column density (this is the difference between the two lines in Figure 1). The dashed box shows the FWHM of the EUVE DS instrument along the energy axis.

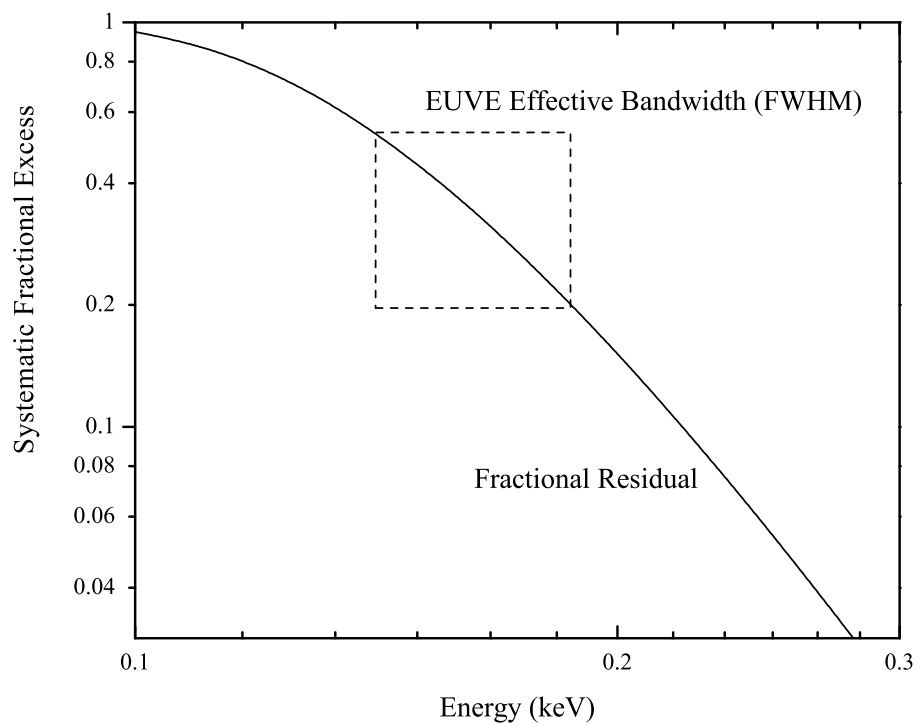


FIG. 9.— The same residual shown in Figure 7, but expressed as the ratio of the residual flux to the model flux when using the average column density. Within the dashed box, which shows the effective bandwidth of the EUVE DS in energy, the residual flux can be 20-60% of the expected flux (a flux-weighted value of about 35%), comparable to the excess soft X-ray emission that has been discussed in the literature.

TABLE 1
GALAXY CLUSTER PROPERTIES

Cluster Name	RA (J2000)	DEC (J2000)	z	L_x (10^{44} erg s $^{-1}$)	T (keV)	N_{HI} (10^{20} cm $^{-2}$)	t_{exp} (ksec)
Abell 119	00:56:16.8	−01:15:00	0.044	3.2	5.6	3.45	15.2
Abell 3376	06:00:43.6	−40:03:00	0.0455	2.1	4.0	4.81	12.0
Abell 2029	15:10:58.7	+05:45:42	0.0767	19.	8.5	3.18	15.6
Abell 2142	15:58:16.1	+27:13:29	0.0899	27.	9.7	3.86	44.2
AWM 4	16:04:55.8	+23:55:54	0.0323	0.30	2.4	5.03	19.9